

High magnetic field properties in $\text{Ru}_{2-x}\text{Fe}_x\text{CrSi}$ with antiferromagnetic and spin-glass statesMasahiko Hiroi,^{*} Sora Nishiinoue, Iduru Shigeta, Masakazu Ito, and Keiichi Koyama*Department of Physics and Astronomy, Graduate School of Science and Engineering, Kagoshima University, Kagoshima 890-0065, Japan*

Akihiro Kondo and Koichi Kindo

Institute for Solid State Physics, The University of Tokyo, Kashiwa 277-8581, Japan

Isao Watanabe

Advanced Meson Science Laboratory, RIKEN Nishina Center for Accelerator-Based Science, Wako, Saitama 351-0198, Japan

Muneaki Fujii

Institute of Pulsed Power Science, Kumamoto University, Kumamoto 860-8555, Japan

Shojiro Kimura

Institute for Materials Research, Tohoku University, Sendai 980-8577, Japan

Hirotaka Manaka and Norio Terada

Department of Electrical and Electronics Engineering, Graduate School of Science and Engineering, Kagoshima University, Kagoshima 890-0065, Japan

(Received 27 June 2018; revised 5 March 2021; accepted 5 March 2021; published 19 March 2021)

We report experimental studies on $\text{Ru}_{2-x}\text{Fe}_x\text{CrSi}$ focusing on properties related to antiferromagnetism in Ru_2CrSi and spin glass (SG) in $\text{Ru}_{1.9}\text{Fe}_{0.1}\text{CrSi}$. By measuring the temperature dependence of magnetization $M(T)$, specific heat $C(T)$, electrical resistivity $\rho(T)$, and muon spin relaxation (μSR), we observed that Ru_2CrSi exhibited an antiferromagnetic (AF) transition at a temperature T_N of ~ 13 K, and $\text{Ru}_{1.9}\text{Fe}_{0.1}\text{CrSi}$ showed SG properties that could be interpreted as successive SG transitions, where the spin-freezing occurred at temperature T_g , and below that strong irreversibility in $M(T)$ and a gradual peak of $M(T)$ at T^* ($>T_g$) appeared. When the data for $0 \leq x \leq 0.1$ were compared, by substituting Fe the AF order was rapidly destroyed and it appeared to change to two anomalies at T^* and T_g . With increasing x , there was a slight change in T_g from T_N for $x = 0$; however, T^* increased, suggesting that the AF and the SG states are closely related. Furthermore, the results of specific heat, resistivity, and magnetization in high fields were presented and compared. For Ru_2CrSi in specific heat under high magnetic fields up to 14 T, the peak shape around T_N and the T_N value were constant. The resistivity and magnetization in pulsed fields suggested that T_N of Ru_2CrSi was constant up to over 50 T. These results demonstrated the unusual robustness of the AF transition to magnetic fields. In $\text{Ru}_{1.9}\text{Fe}_{0.1}\text{CrSi}$, unusual hysteresis in magnetoresistance was observed in static and pulsed magnetic fields, although their appearances differed. These hystereses were considered a manifestation of the curious properties of the SG state with strong irreversibility.

DOI: [10.1103/PhysRevB.103.094428](https://doi.org/10.1103/PhysRevB.103.094428)**I. INTRODUCTION**

Half-metals are ferromagnetic metals with a density of states in only one spin channel, and there is a gap in the other spin channel at the Fermi energy, implying 100% spin-polarized conduction electrons [1–3]. Some Heusler compounds are considered half-metals [1,3], and this is partly why Heusler compounds have become a research hot spot recently. They have a chemical formula of X_2YZ , where X and Y are transition metal elements, and Z is an sp element. The structure is such that four fcc lattices comprising each element

penetrate each other. A band-structure calculation predicted that the Heusler compound $\text{Ru}_{2-x}\text{Fe}_x\text{CrSi}$ is a complete or a nearly complete half-metal that is robust to chemical disorder for a wide range of x [4]. We have studied the properties of the Heusler compounds $\text{Ru}_{2-x}\text{Fe}_x\text{CrSi}$ experimentally: observably, the Fe-rich compounds are ferromagnetic and half-metal candidates [5,6]. Meanwhile, the Ru-rich compounds are also important. The end compound Ru_2CrSi showed an antiferromagnetic (AF) transition at $T_N \sim 13$ K indicated by the peak of the temperature dependence of magnetization $M(T)$ and that of the specific heat $C(T)$ [7,8]. In the temperature dependence of the electrical resistivity $\rho(T)$ of Ru_2CrSi , a dip was observed at T_N . From the $\rho(T)$ measurement for different values of magnetic field B up to 14.5 T, T_N was found to

^{*}hiro@sci.kagoshima-u.ac.jp

hardly depend on B , conforming to $M(T)$ measurements for different B below 7 T [8]. These facts demonstrated that the low-temperature phase of Ru_2CrSi is an AF state, although no microscopic evidence exists for the AF order yet. Meanwhile, $\text{Ru}_{2-x}\text{Fe}_x\text{CrGe}$ was revealed to be almost magnetically identical to $\text{Ru}_{2-x}\text{Fe}_x\text{CrSi}$ [9], and in Ru_2CrGe , an AF order was confirmed by a neutron diffraction measurement [10]. While a band-structure calculation in $\text{Ru}_{2-x}\text{Fe}_x\text{CrSi}$ showed that the half-metallic state, which is in principle a ferromagnetic state, was predicted for a wide range of x , antiferromagnetic states are energetically more favorable than the ferromagnetic state for small x .

Although the Ru-rich compound $\text{Ru}_{1.9}\text{Fe}_{0.1}\text{CrSi}$ showed a peak in $M(T)$ around 30 K, where the temperature is referred to as T^* , this peak indicated no AF transition, contrary to the case in Ru_2CrSi . In specific heat, no anomaly or jump was detected, indicating that a phase transition did not occur [11,12]. According to our muon spin relaxation (μSR) study, around T^* , a gradual formation of an inhomogeneous magnetic state comprising small spin-frozen regions started [13], and spin freezing occurred at a lower temperature of ~ 15 K. Moreover, a clear kink in $M(T)$ was observed in a zero-field cooling (ZFC) process, which means that below this temperature, irreversibility in $M(T)$, that is, the difference in $M(T)$ between a ZFC and a field-cooling (FC) process, is enhanced. This temperature is defined as T_g . Although T_g depends rather largely on magnetic fields in the low-field region, its value extrapolated to $B = 0$ is ~ 15 K, which agrees with the spin-freezing temperature found by μSR . So, it is considered that at T_g spin-freezing occurs, and below T_g strong irreversibility appears. Nevertheless, irreversibility in $M(T)$ between ZFC and FC begins at higher temperature around T^* and is called weak irreversibility. These results are regarded as spin-glass (SG) behavior characterized by spin-freezing and an inhomogeneous magnetic state. This SG behavior interpreted as successive SG transitions has been reported [11], and it needs to be investigated further.

Transport properties of Ru_2CrSi and $\text{Ru}_{1.9}\text{Fe}_{0.1}\text{CrSi}$ in high magnetic fields are also important. In $\rho(T)$ of Ru_2CrSi a clear kink was observed at T_N for different B up to 14.5 T. These data imply that T_N is hardly changed by a magnetic field up to 14.5 T [8]. Conversely, $\text{Ru}_{1.9}\text{Fe}_{0.1}\text{CrSi}$ exhibits semi-conducting behavior in $\rho(T)$, namely a monotonic increase with a decrease in temperature, and no anomaly indicating transitions. This behavior differs from the metallic behavior of the Fe-rich compounds or the characteristic temperature dependence of Ru_2CrSi . In a magnetic field, negative magnetoresistance (MR) was observed [11,14]. These results imply that only a small amount of Fe substitution has a considerable effect on the magnetic and magnetotransport properties. Also in $\text{Ru}_{2-x}\text{Fe}_x\text{CrSi}$ ($x = 0.3$ and 0.5), negative MR was observed.

Therefore, in this study, magnetization, specific heat, magnetoresistance, and muon spin relaxation experiments were conducted to explore the relationship between the AF state of Ru_2CrSi and the SG state of $\text{Ru}_{1.9}\text{Fe}_{0.1}\text{CrSi}$. Then, we investigated their magnetization and electrical resistivity under high magnetic field using static and pulsed fields, focusing on the change in T_N of Ru_2CrSi in a high field and the hysteresis in MR in $\text{Ru}_{1.9}\text{Fe}_{0.1}\text{CrSi}$.

II. EXPERIMENTS

Polycrystalline samples of $\text{Ru}_{2-x}\text{Fe}_x\text{CrSi}$ ($0 \leq x \leq 0.5$) were prepared by arc-melting high-purity constituent elements under a high-purity argon atmosphere. Nominal Fe concentration x shows the amount at the preparation. Although for low x it might not be very correct, the properties show a reasonable systematic dependence on x . Crystal structures were examined using x-ray powder diffraction measurements with Cu $K\alpha$ radiation. We confirmed that the prepared samples were practically single phase, although a few extra peaks were observed in samples with small x ($\lesssim 0.01$). The crystal structure, x-ray diffraction patterns, and the lattice constants for $x = 0$ and $0.1 \leq x \leq 1.8$ are depicted in [11,15]. The lattice constant of Ru_2CrSi was 0.588 nm [15], and the lattice constants for $0 < x < 0.1$ as a function of x were interpolated. Magnetization and magnetoresistance were measured using commercial measurement systems (MPMS and PPMS; Quantum Design). High-field magnetization was measured by the induction method using a standard pick-up coil in pulsed magnetic fields. Pulsed magnetic fields up to 72 T were generated with a duration time of several milliseconds (ms) using nondestructive magnets. The absolute value was calibrated by comparing the data with the magnetization below 7 T measured using MPMS. High-field magnetoresistance up to ~ 55 T was measured using the usual four-probe method with a pulsed magnetic field of a duration time of several tens of ms. High-field magnetoresistance was also measured under static magnetic fields using superconducting magnets up to 18 T and a ^3He cryostat. Specific heat was measured by the usual adiabatic method at 0 T and the relaxation method in a magnetic field up to 14 T using a PPMS. Measurements of μSR were performed at the RIKEN-RAL Muon Facility [16] using a spin-polarized single-pulse positive surface muon (μ^+) beam with a momentum of 27 MeV/c.

III. RESULTS

A. Magnetization and resistivity of $\text{Ru}_{2-x}\text{Fe}_x\text{CrSi}$ ($0 \leq x \leq 0.1$)

First, we describe the basic properties such as magnetization and resistivity of $\text{Ru}_{2-x}\text{Fe}_x\text{CrSi}$, focusing on the compounds with $0 \leq x \leq 0.1$. The comprehensive studies including larger x [5,6,9,11] and a preliminary study for $0 \leq x \leq 0.1$ [7] have been reported. Figure 1(a) shows $M(T)$ for $0 \leq x \leq 0.05$ at $B = 1$ T. In $M(T)$ measurement for $0 < x \leq 0.1$, essentially the same behavior as for $x = 0.1$ was observed: the peak in $M(T)$ at T^* and a kink in $M(T)$ for ZFC at T_g , below which M decreases rapidly, and thus the irreversibility between ZFC and FC is enhanced. For $x = 0.1$, T_g is ~ 6 K and T^* is ~ 30 K at $B = 1$ T, as reported [11]. With a decrease in x , T_g appears constant, whereas T^* decreases and appears to tend to ~ 13 K, which is T_N for $x = 0$ [Fig. 1(a)]. Notably, with the increase in x , the magnitudes of M and T^* increase. From the $B - T$ phase diagram (shown later), for $x = 0.1$ and 0.02 , T_g depends on B rather largely in the low- B region [7,11], and it appears to approach ~ 15 K to the low-field limit ($B \rightarrow 0$), while T^* slightly depends on magnetic field. Although for $x = 0$ the peak of $M(T)$ at ~ 13 K exhibits the AF transition, the peak is small. The temperature dependence of $M(T)$ up to room temperature is weak, and it causes a large negative Weiss

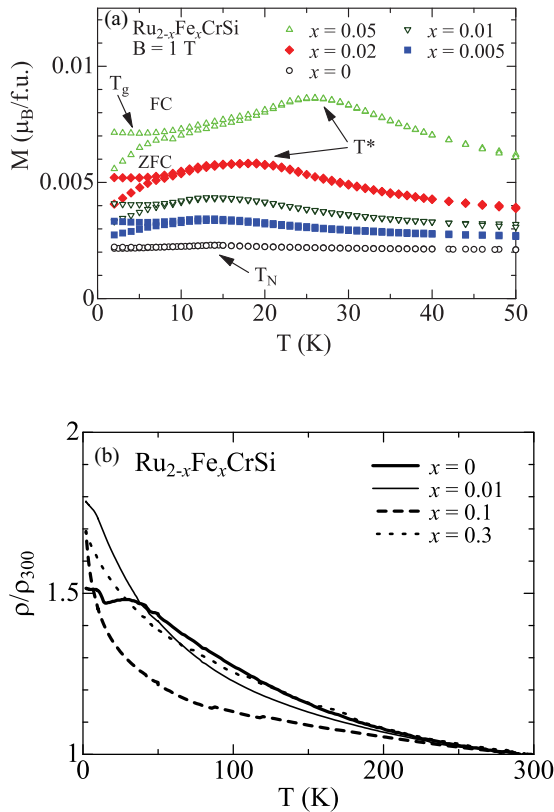


FIG. 1. (a) Temperature dependence of the magnetization $M(T)$ at a magnetic field of 1 T of $\text{Ru}_{2-x}\text{Fe}_x\text{CrSi}$ ($0 \leq x \leq 0.05$). Irreversibility between zero-field cooling (ZFC) and field cooling (FC) is observed. (b) Typical temperature dependences of the resistivity normalized by that at 300 K, $\rho(T)/\rho_{300}$ of $\text{Ru}_{2-x}\text{Fe}_x\text{CrSi}$ ($0 \leq x \leq 0.3$).

temperature of -945 K, which is considered to indicate large frustration in the magnetic interactions [15], which probably causes the small and less conspicuous peak in $M(T)$ at T_N . Additionally, T^* and T_g become close for $x \simeq 0$, and $M(T)$ even for $x = 0$ shows a slight irreversibility. For these reasons, it is difficult to clearly differentiate the behavior of $M(T)$ for $x = 0$ and low x (≤ 0.01).

Figure 1(b) shows typical temperature dependences of the resistivity normalized at 300 K, $\rho(T)/\rho_{300}$ of $\text{Ru}_{2-x}\text{Fe}_x\text{CrSi}$ ($0 \leq x \leq 0.3$). They show basically semiconducting behavior, that is, $\rho(T)$ increases with a decrease in T , in contrast to metallic behavior for larger x [6,11]. For $x = 0$, a dip that indicated the AF transition (at T_N) was observed, and below the dip temperature, the increase in $\rho(T)$ with a decrease in temperature was suppressed. For $x = 0.01$, a slight Fe substitution canceled the dip in $\rho(T)$, and an increase in $\rho(T)$ toward $T = 0$ was detected, similar to $x = 0.1$. We observed the absence of the dip in $\rho(T)$ even for $x = 0.005$, demonstrating that only a slight Fe substitution destroyed the AF order, although it appeared unclear in $M(T)$. Nevertheless, a suppressed increase in $\rho(T)$ below ~ 10 K was observed for $x = 0.01$, which might reflect an AF correlation development observed similarly in the specific heat (as described later). For $x = 0.1$, a monotonic increase was observed in $\rho(T)$ toward low temperature without an anomaly indicating a transition, and it showed an almost perfect $\ln T$ dependence

for a wide temperature range from 1.5 to 300 K [14,17]. However, whether the $\ln T$ dependence is accidental is unclear. For $x = 0.3$ the temperature dependence becomes weaker, and the magnitude of ρ decreases toward metallicity. The main origin of semiconducting behavior for small x is probably the decrease in the carriers, though it is not thermally activated behavior. By considering the magnetoresistance results described later, randomness and magnetic scattering caused by Fe yield this semiconducting behavior, and the AF correlation complicates the behavior.

B. Specific heat

Figure 2(a) shows the specific heat $C(T)$ of $\text{Ru}_{2-x}\text{Fe}_x\text{CrSi}$ ($x = 0, 0.01, \text{ and } 0.1$). Some $C(T)$ data up to $x = 0.5$ have been reported [7,11,12], and the present data are analyzed similarly. Specific heat comprised three components: the lattice specific heat C_l , electronic specific heat C_e , and magnetic specific heat C_m . As described in [12], the lattice contributions in a low-temperature region for $T < 100$ K were estimated from $\text{Ru}_{0.4}\text{Fe}_{1.6}\text{CrSi}$ with a relatively high Curie temperature T_C of 500 K, implying that C_m was small enough at temperatures far below T_C , and the assumption that the lattice contribution slightly depended on x was reasonable. The estimated $C_l(T)$ is displayed by the dotted line in Fig. 2(a), having the Debye form of a T^3 dependence at low temperatures with a Debye temperature of 496 K. As explained later, the remained specific heat obtained by subtracting the lattice contribution was considered magnetic specific heat $C_m(T)$ [$= C(T) - C_l(T)$], as shown in Fig. 2(b) in the form of C_m/T versus T . The inset shows an enlarged view of this at low temperatures. This shows that C_m/T is proportional to T and the extrapolation to 0 K intersects the origin, that is, $C(T)$ has no linear T term and is proportional to T^2 at low temperatures. The former shows no electronic contribution in these compounds within the experimental resolutions, and this conforms to not-metallic behavior of these compounds. Note that the linear T contribution was observed for $x = 0.3$ and 0.5 , regarded as C_e , and reflected increasing metallicity with an increase in x [6,11,12]. Consequently, we can see that in $C(T)$ of these compounds there is no electronic contribution, and the remaining specific heat obtained by subtracting the lattice contribution can be attributed to a magnetic contribution.

Even though the peak in $M(T)$ at T_N for $x = 0$ is less conspicuous, a clear peak in $C(T)$ is observed at 13 K [Fig. 2(a)], which is firm evidence of a thermodynamic transition. Although the sharpness and the magnitude of the peaks are slightly dependent on samples, a clear peak is observed at 13 K for all measured samples [Fig. 3(a)]. Meanwhile, for $x = 0.1$, no discontinuous anomaly is observed around T_g , T_N , or at any temperatures, suggesting no phase transition. Nevertheless, a round peak in C_m/T was observed as in conventional SG, whereas a linear T term in specific heat, which is often observed in conventional SG, was unrecognized. Instead, T^2 specific heat was observed along with the other compounds for $0 \leq x \leq 0.5$ [12], which means the AF state is not responsible for this dependence. In frustrated and random systems, T^2 specific heat has been reported [18,19]. Meanwhile, for $x = 0.01$, although a distinct peak in $C(T)$ was unobserved, an anomaly at ~ 12 K was clearly observed, which is more

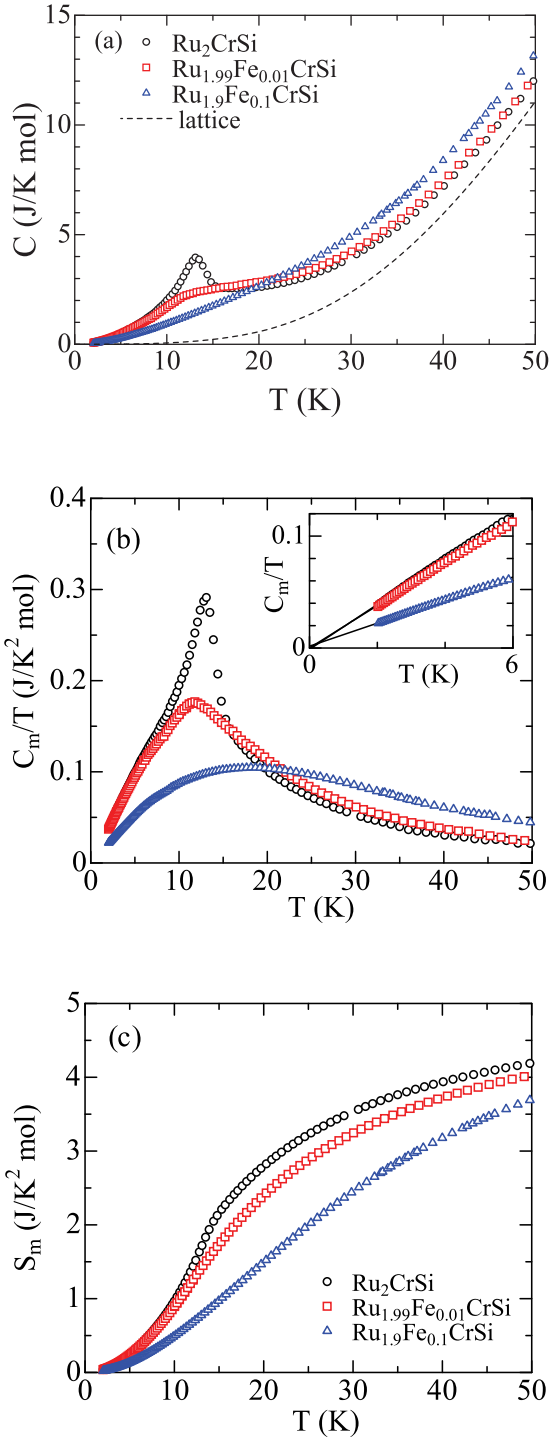


FIG. 2. (a) Specific heat $C(T)$ of $\text{Ru}_{2-x}\text{Fe}_x\text{CrSi}$ ($x = 0, 0.01$, and 0.1). The dotted line shows the estimated lattice contribution (see the text). (b) Magnetic specific heat divided by T , $C_m(T)/T$, $C_m(T)$ is obtained by subtracting the lattice contribution. The inset is an expanded view at low temperatures. An absence of a linear term and a T^2 dependence of $C_m(T)$ at low temperatures are observed. (c) Magnetic entropy S_m obtained by integrating (b).

clearly detected as a peak in C_m/T versus T in Fig. 2(b). The anomaly is slightly below T_N for $x = 0$, accounted for by the randomness that degrades long-range order. This shows

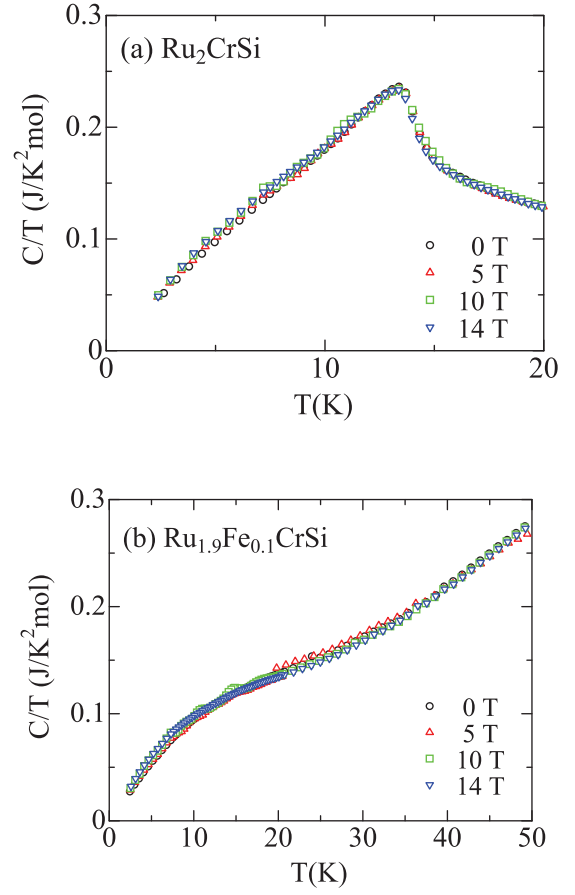


FIG. 3. Specific heat, as a form of $C/T - T$, of the $\text{Ru}_{2-x}\text{Fe}_x\text{CrSi}$ [$x = (a) 0$ and (b) 0.1] under magnetic fields of 0, 5, 10, and 14 T. For both samples at any fields up to 14 T, no influence of magnetic field is observed.

that the AF correlation holds up to $x \simeq 0.01$ even though Fe substitution destroys the AF order.

Figure 2(c) shows the magnetic entropy obtained by integrating C_m/T . For approximately 50 K, the entropy reached around 4 (J/K²mol) and continued to increase gradually, particularly for $x = 0.1$. This is considerably below 5.76 (J/K²mol) ($=R \ln 2$), which is the value if we assume 1/2 spin resides at each Cr site. This suggests the role of itinerancy and frustration.

Figure 3 show the specific heat for $x = 0$ and 0.1 in a magnetic field up to 14 T. For both compounds, the $C(T)/T$ curves for different magnetic fields agree with each other. We can say that the specific heat is completely independent of magnetic field up to 14 T within experimental resolution. For $x = 0$, even at 14 T, both the transition temperature and the peak shape remained constant, suggesting the robustness of the transition toward a much higher magnetic field. This will be clarified through measurements in the pulsed high field. Furthermore, such unchanged specific heat around T_N with respect to the magnetic field was reported for other materials [20–22].

According to the Maxwell relation,

$$\frac{\partial S}{\partial B} = \frac{\partial M}{\partial T}. \quad (1)$$

From $M(T)$ at $B = 1$ T, $|\partial M/\partial T|$ is $\lesssim 10^{-5}$ (J/K T f.u.) for $x = 0$ and $\lesssim 10^{-4}$ (J/K T f.u.) for $x = 0.1$. As presumed from Fig. 2(c), the field dependence of the entropy is considered almost absent within the experimental resolution. The independence of the specific heat on magnetic field conforms to the weak temperature dependence of $M(T)$.

C. μ SR of Ru_2CrSi

We have performed muon spin relaxation studies, and the results for $x = 0.1$ have been reported [13]. We investigated zero-field muon spin relaxation (ZF- μ SR) measurements and longitudinal-field muon spin relaxation (LF- μ SR) measurements in a longitudinal field of 0.01 T for Ru_2CrSi . Observably, the obtained results for LF- μ SR were essentially the same as those for ZF- μ SR, although this field was applied to decouple the nuclear spin contribution and to extract the electron spin effects. In μ SR measurements, spin-polarized muons are implanted into samples. The muon spin depolarization due to internal fields at the muon sites is described by the asymmetry $A_0(t)$ defined as follows:

$$A_0(t) = \frac{F(t) - \alpha B(t)}{F(t) + \alpha B(t)}. \quad (2)$$

Here $F(t)$ and $B(t)$ are the total muon events counted by the forward and backward counters at time t , respectively, and α is a calibration factor reflecting relative counting efficiencies between the forward and backward counters.

Figure 4(a) shows the LF- μ SR time spectra of the asymmetry $A_0(t)$ in Ru_2CrSi at temperatures between 2 and 30 K. The relaxations were well fitted by a single exponential function:

$$A_0(t) = A \exp(-\lambda t), \quad (3)$$

where A is the initial asymmetry and λ is the muon relaxation rate. Figure 4(b) shows the obtained A and λ . The conspicuous change in A between 10 and 20 K indicates the development of an ordered state. The midpoint of the change in A is about 15 K, which is reasonably considered to be T_N [23]. A peak in λ was observed around this temperature, indicating a critical slowdown. This behavior shows that a phase transition in magnetic origin occurs around 15 K in terms of μ SR. However, an oscillatory signal by the internal field of the AF order was unobserved, possibly due to a large internal field.

D. Magnetization in high field

Figure 5 shows magnetization as a function of magnetic field $M(B)$ up to $B = 72$ T at 4.2 K for $\text{Ru}_{2-x}\text{Fe}_x\text{CrSi}$ ($x = 0, 0.1, 0.3, \text{ and } 0.5$). In Ru_2CrSi , which is in the AF state at zero field, the $M(B)$ curve is almost a perfect straight line up to 72 T, suggesting no transition, and the AF state persists up to the highest magnetic field. For $x = 0.1$, the $M(B)$ curve is convex in a relatively low-field region, reflecting SG nature, and in a higher-field region $M(B)$ increases almost linearly with B and shows no tendency to saturation. Notably, the $M(B)$ curves for $x = 0$ and 0.1 measured at 1.4 K are the same as those at 4.2 K within the experimental resolution. No hysteresis between increasing and decreasing B was observed for both 1.4 and 4.2 K. This is critical when we compare with the magnetoresistance results in a pulsed field. However,

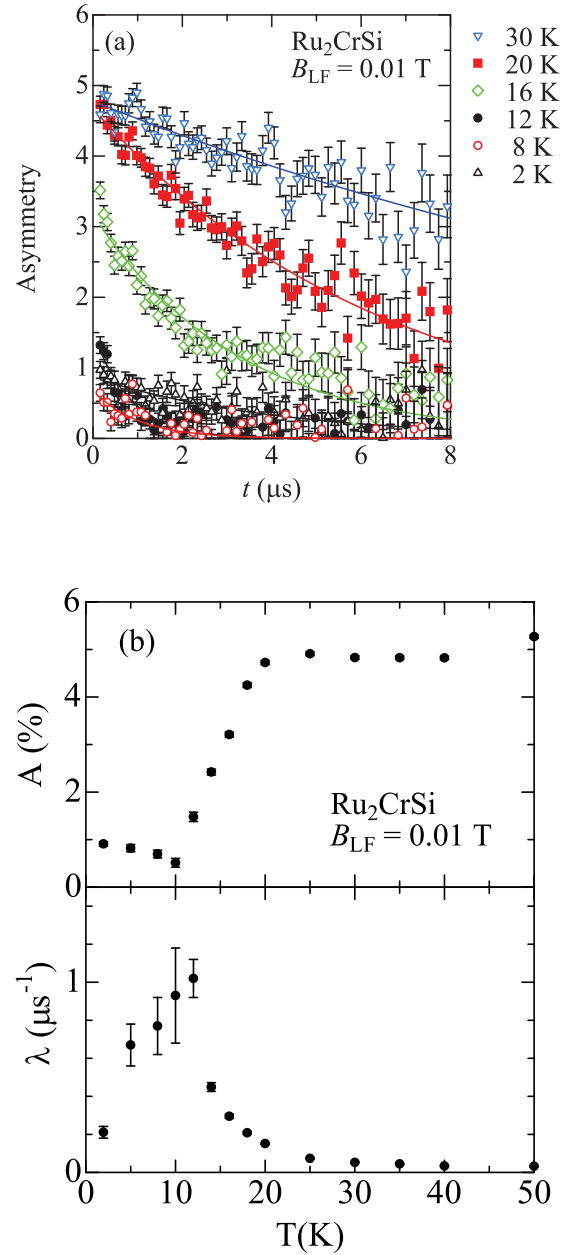


FIG. 4. (a) Time spectra of the asymmetry in μ SR of Ru_2CrSi at longitudinal field $B_{\text{LF}} = 0.01$ T at various temperatures. Solid lines are fit to a single exponential function [Eq. (3)]. (b) Temperature dependence of the initial asymmetry A and the relaxation rates λ after zero-field cooling.

in static fields, the hysteresis in $M(B)$, probably due to the SG state development, was observed at low temperatures, as reported in [11], although it is small and therefore it is not strange that it was unobserved in pulsed fields. For $x = 0.3$ and 0.5, M initially increases rapidly from $B = 0$, reflecting the ferromagnetism. In the higher-field region, M increases gradually and also shows no tendency to saturation up to 70 T. The magnetization per formula unit at 70 T for $x = 0.5$ is approximately $0.8\mu_B$. This is considerably below $2\mu_B$, which was the theoretically predicted spontaneous magnetization independent of a wide range of x [4], and the experimen-

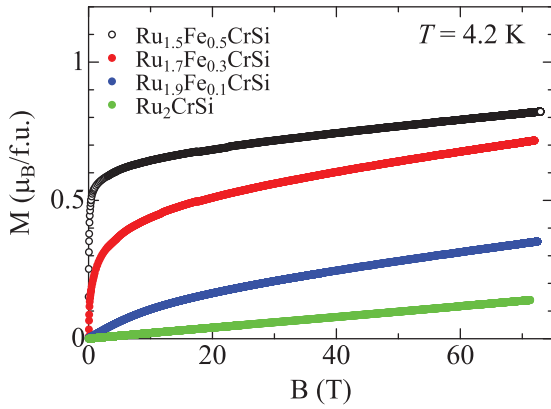


FIG. 5. Magnetization of $\text{Ru}_{2-x}\text{Fe}_x\text{CrSi}$ ($x = 0, 0.1, 0.3, \text{ and } 0.5$) in pulsed fields up to $B = 72$ T at 4.2 K.

tally obtained spontaneous magnetization of $\sim 2\mu_B$ for higher $x \sim 2$, indicating that itinerancy is critical to the magnetism of these compounds.

Figure 6 shows $M(B)$ for Ru_2CrSi up to 55 (72) T at temperatures between 1.4 and 20 K, that is, from low temperatures much below T_N to temperatures sufficiently higher than T_N (at $B = 0$). These $M(B)$ curves are also straight up to the highest magnetic field and are identical to each other within the experimental resolution, conforming to the weak temperature dependence of $M(T)$. Almost complete straight lines of $M(B)$ show no indication of transitions and imply that the AF state persists up to high fields. Even at temperatures slightly below T_N , where the transition field is expected to be low, the $M(B)$ line does not appear to cross the transition, suggesting that the AF transition line in the $B - T$ phase diagram is almost upright (shown later in Fig. 11).

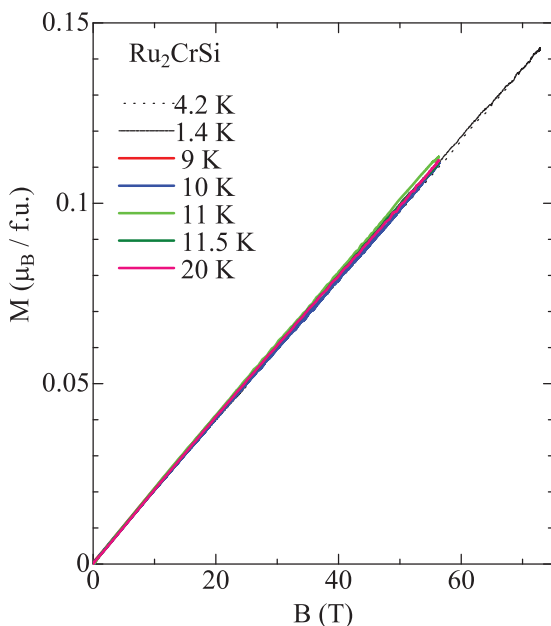


FIG. 6. Magnetization of Ru_2CrSi in pulsed fields at temperatures $4.2 \leq T \leq 20$ K.

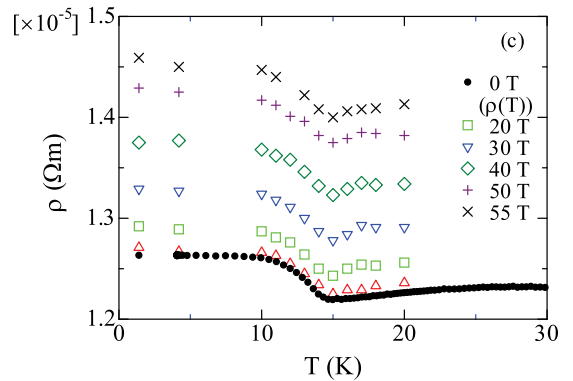
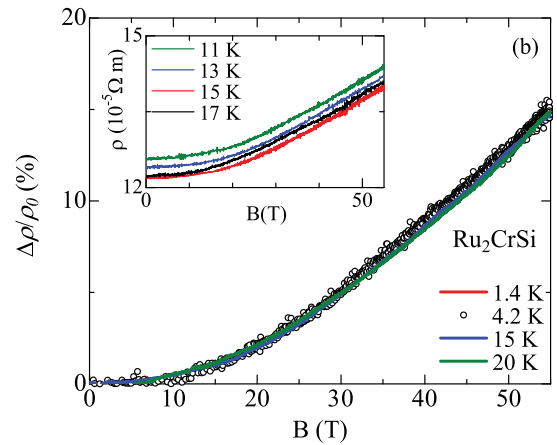
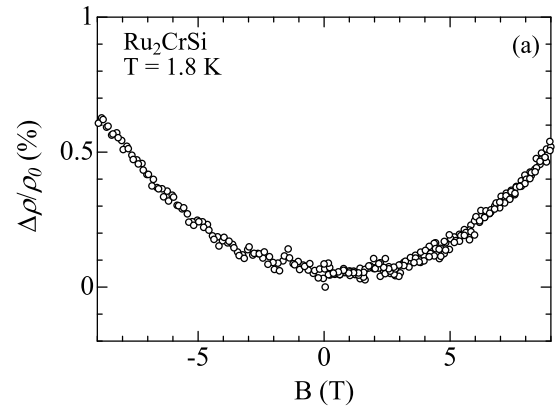


FIG. 7. (a) Magnetoresistance ratio $\Delta\rho(B)/\rho_0$ of Ru_2CrSi at $T = 1.8$ K in static magnetic fields. (b) $\Delta\rho(B)/\rho_0$ of Ru_2CrSi in pulsed fields at temperatures of $1.4 \leq T \leq 20$ K. (c) Temperature dependence of resistivity for different values of magnetic field constructed from the $\rho(B)$ data in pulsed fields at different temperatures, shown in (b). Solid circles show the data of $\rho(T)$ at $B = 0$ measured directly for this sample with varying temperature.

E. Magnetoresistance

Figure 7(a) shows the magnetoresistivity ratio (MRR) $\Delta\rho(B)/\rho_0 = [\rho(B) - \rho_0]/\rho_0$ for Ru_2CrSi at 1.8 K in static fields with varying B as $0 \rightarrow 9 \rightarrow -9 \rightarrow 0$ T, where $\rho(B)$ and ρ_0 are resistivities at the temperature in a magnetic field of B and in zero magnetic field, respectively. Figure 7(b)

shows the high-field MRR up to 55 T measured using pulsed magnetic fields at temperatures between 1.4 and 20 K. The range includes T from far lower than $T_N = 13$ K at $B = 0$ to T higher than that. From the figures, basically the same behaviors were observed under pulsed and static fields, and they are independent of temperature. The magnetic field dependences can be approximately described as $\Delta\rho(B)/\rho_0 = \alpha B^2$ up to the highest field, 55 T, and α is estimated to be 5.9×10^{-3} ($\%/T^2$). The $\rho(B)$ curves all look similar, and one curve appears to overlap just with others by shifting in parallel, as displayed in the inset of Fig. 7(b). In those $\rho(B)$ curves, no sign of the transition was observed, despite the characteristic change in $\rho(T)$ around T_N . Notably, no hysteresis in $\rho(B)$ between increasing and decreasing B was observed even at low temperatures for both pulsed and static fields, in contrast to the case for $x = 0.1$, described later.

From these data, we have constructed the temperature dependence of ρ for different values of magnetic fields by adding $\Delta\rho(B)$ to $\rho(T)$ at $B = 0$, which was measured directly for the present sample [Fig. 7(c)], and a clear dip indicating that the AF transition was observed at ~ 15 K, which agrees with that in Fig. 1(b). Consequently, from Fig. 7(c), at different magnetic fields, the dip exists and no shift in T_N is observed. From the inset of Fig. 7(b), it can be seen that the identity of the $\rho(B)$ curves in parallel shifts shows that the temperature of the dip in $\rho(T)$ remains constant when the magnetic field is changed. Considering the results for $\rho(T)$ under 14.5 T measured in static fields [13], and for specific heat up to 14 T, we have clearly observed that T_N appears to be constant even in fields as high as 55 T.

Figure 8(a) shows the MRR of $\text{Ru}_{1.9}\text{Fe}_{0.1}\text{CrSi}$ at temperatures between 1.8 and 10 K. Figure 8(b) shows the MRR of Fe-substituted samples with $x = 0.06, 0.3$, and 0.5 at 2 K. These measurements start initially in a ZFC condition with B varying as $0 \rightarrow 9 \rightarrow 0 \rightarrow -9 \rightarrow 0 \rightarrow 9 \rightarrow 0$ T, as indicated by arrows 1–7, and ρ_0 is the value of $\rho(0)$ when B returns to zero from 9 T. For $x = 0.1$, MR is negative and the hysteresis appears below 4 K. The hysteresis in $\rho(B)$ observed at 4 K makes a symmetric loop centered at ρ_0 ($B = 0$). The loop-type hysteresis seems relevant to weak irreversibility found in SG states, some ferromagnetic systems, or in inhomogeneous magnetic states [24–26], and it is also seen for $x = 0.3$, as shown in Fig. 8(b). Note that, for $x = 0.5$, although the hysteresis in $\rho(B)$ almost disappears, it still remains in $M(B)$, and for larger x the hysteresis tends to disappear as the compound becomes a homogeneous soft ferromagnet [5,11]. However, different behaviors occur for 1.8 and 2.2 K, as shown in Fig. 8(a). The initial $\Delta\rho(B)/\rho_0$ for B increasing from 0 T after ZFC (arrows 1 and 2) differs from the curve obtained by the sequence shown by arrows 3–7. It starts at 0 T from a value below ρ_0 (arrow 1), and with increasing field (arrow 2) it meets the curve obtained in the following sequence, and the loop repeats. The magnetic field where the initial $\rho(B)$ curve after ZFC meets the loop in the subsequent sequence is represented as B_i . For $x = 0.06$, the same type of unusual hysteresis pattern in $\rho(B)$ occurs as for $x = 0.1$ [Fig. 8(b)]. This compound exhibits practically the same magnetic behavior with strong irreversibility below T_g as for $x = 0.1$. Therefore, the unusual hysteresis observed after ZFC for $x = 0.1$ (and

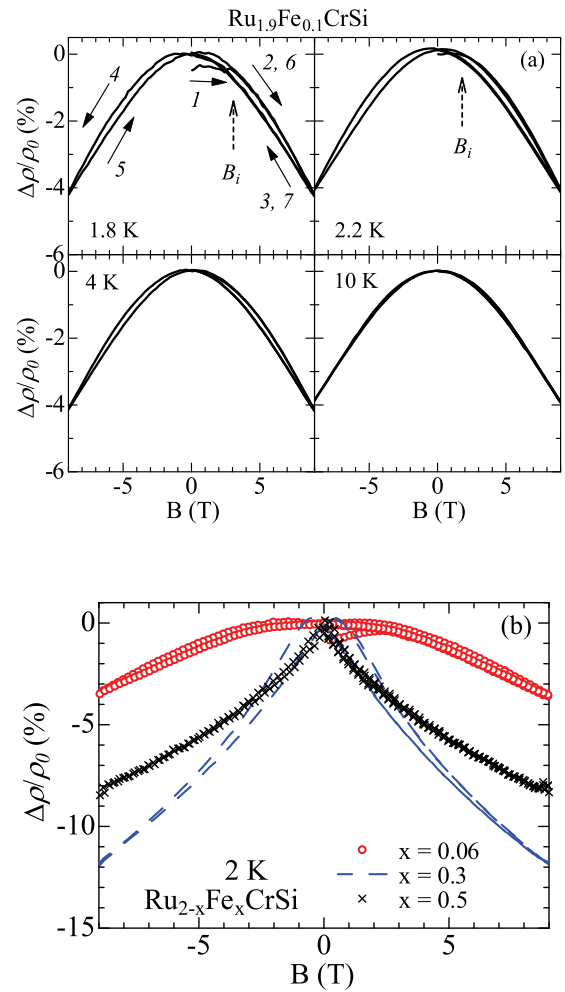


FIG. 8. (a) Magnetoresistance ratio $\Delta\rho(B)/\rho_0$ of $\text{Ru}_{1.9}\text{Fe}_{0.1}\text{CrSi}$ under a static field. The arrows show the order of varying magnetic field. The measurements start initially in a zero-field-cooling (ZFC) condition, and ρ_0 is the value of $\rho(0)$ when B returns to zero from 9 T. B_i is the magnetic field where the initial $\rho(B)$ curve after ZFC, indicated by the arrow 1, meets the loop of $\rho(B)$ in the subsequent sequence. (b) $\Delta\rho(B)/\rho_0$ of $\text{Ru}_{2-x}\text{Fe}_x\text{CrSi}$ as a function of magnetic field with $x = 0.06, 0.3$, and 0.5 at 2 K, measured under a static magnetic field up to 9 T with the field sequence shown in (a) after ZFC.

$x = 0.06$) is exceptional and relevant to the strong irreversibility that accompanies the SG state.

Furthermore, we measured the MR for $x = 0.1$ under higher static magnetic fields. Figure 9(a) shows the MRR measured at 1.3 K initially in ZFC followed by varying B with $0 \rightarrow 18 \rightarrow 0$ T for transverse and longitudinal geometries. The unusual hysteresis behavior appears at 1.3 K, as shown in the inset of Fig. 9(a). One possible factor affecting MR behavior is the measurement geometry, that is, a longitudinal or a transverse geometry. However, the data for both configurations agree perfectly with each other. Figure 9(b) shows the MRR for $x = 0.1$ at 0.5 K initially in a ZFC condition, followed by the field cycle of $0 \rightarrow 10 \rightarrow 0 \rightarrow -10 \rightarrow 0 \rightarrow 10 \rightarrow 0$ T. On the whole, the behavior is the same as that for 1.3 K, although B_i was not as different as for 1.3 K,

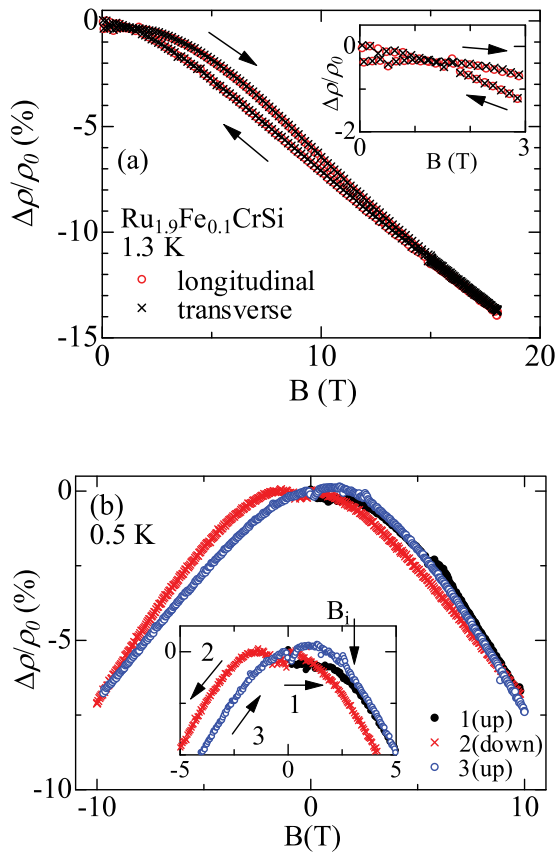


FIG. 9. (a) Magnetoresistance ratio $\Delta\rho(B)/\rho_0$ of $\text{Ru}_{1.9}\text{Fe}_{0.1}\text{CrSi}$ under a static field at $T = 1.3$ K after ZFC from 0 to 18 T and decreasing B back to 0 T for longitudinal and transverse configurations. The inset shows an expanded view around 0 T. The arrows show the order of varying magnetic field: first increasing B after ZFC and decreasing B back to 0 T. (b) $\Delta\rho(B)/\rho_0$ of $\text{Ru}_{1.9}\text{Fe}_{0.1}\text{CrSi}$ under a static field at $T = 0.5$ K in varying B back and forth for $-10 \leq B \leq 10$ T from 0 T after ZFC. The arrows show the order of varying magnetic field. The inset shows an expanded view around $B = 0$ T.

contrary to the tendency to increase with decreasing temperature (Fig. 11). Note that the ZFC condition might not be realized as strictly as at $T \gtrsim 1.3$ K because temperature control is difficult.

Using a pulse magnet, the high-field MR of $\text{Ru}_{1.9}\text{Fe}_{0.1}\text{CrSi}$ up to 56 T was measured at temperatures between 1.4 and 30 K. Figure 10(a) shows $\rho(B)$ for increasing and subsequent decreasing B after ZFC. Although the data shown here have been averaged and smoothed, the feature of $\rho(B)$ discussed here was unaltered. The resistivity of this sample at $B = 0$ T is approximately $1.2 \times 10^{-3} \Omega \text{ cm}$ at $T = 4.2$ K and $0.94 \times 10^{-3} \Omega \text{ cm}$ at $T = 30$ K [11, 14]. The curves in Fig. 10(a) are shifted for clarity. The sequential changes in B are represented by arrows. $\rho(B)$ exhibits no sign of saturation and changes almost linearly in the higher-field region. The MRR becomes approximately -30% at 55 T and its magnitude slightly depends on temperatures below 30 K, as obtained under static fields [14].

However, from Fig. 10(a), the most prominent feature is an unusual hysteresis that occurs as a function of B at low

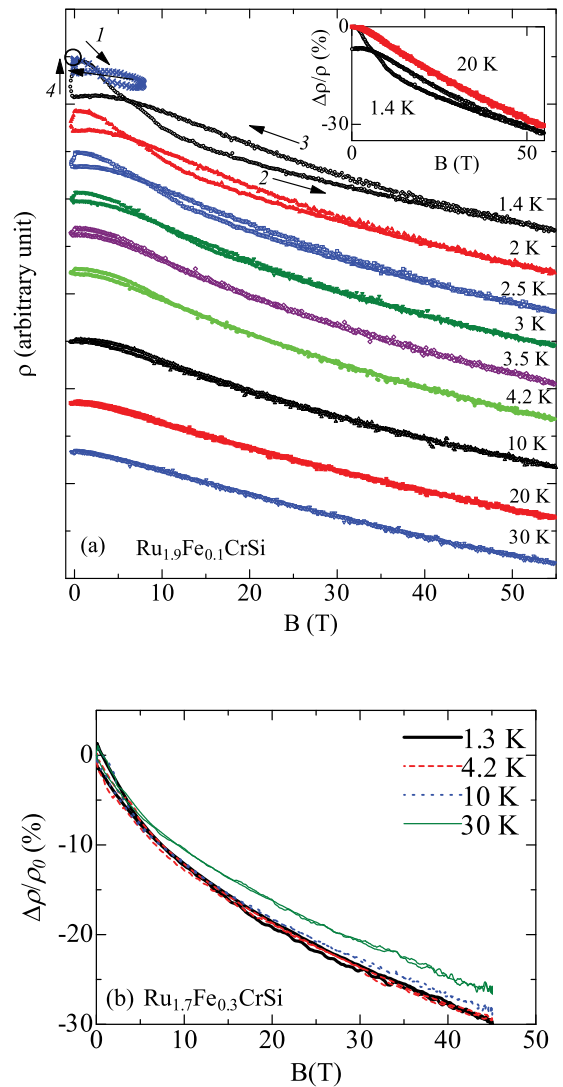


FIG. 10. (a) Electrical resistivity of $\text{Ru}_{1.9}\text{Fe}_{0.1}\text{CrSi}$ under pulsed fields of $B = 56$ T as a function of magnetic field B at temperatures between 1.4 and 30 K. The curves are offset by equal amounts for clarity. The inset shows the magnetoresistance ratio (MRR) $\Delta\rho(B)/\rho_0$ at 1.4 and 20 K. The magnitude of MRR hardly changes below 30 K. For the data at 1.4 K, the open circle shows the starting point and the arrows show the time ordering of B . Crosses show MR for a smaller pulsed field of 7.8 T at 1.4 K. For $T \lesssim 3$ K, an unusual hysteresis appears, forming a figure-8. (b) MRR of $\text{Ru}_{1.7}\text{Fe}_{0.3}\text{CrSi}$ under pulsed fields of $B = 45$ T at temperatures between 1.3 and 30 K.

temperatures (below ~ 3 K). This becomes more remarkable at lower temperatures, as shown for 1.4 K by the arrows. At 4.2 K, the hysteresis is almost completely unclear, and around 10 K it disappears altogether. The MR curve at 1.4 K for increasing B just after ZFC begins from the point indicated by the open circle in Fig. 10(a). The return $\rho(B)$ curve for decreasing B (arrow 2), intersects the curve (at ~ 8 T for the 56 T pulse), and then returns at ~ 0 T below the starting point. Then it returns to the starting point in approximately 5 ms after the pulsed field becomes zero field (arrow 4), probably

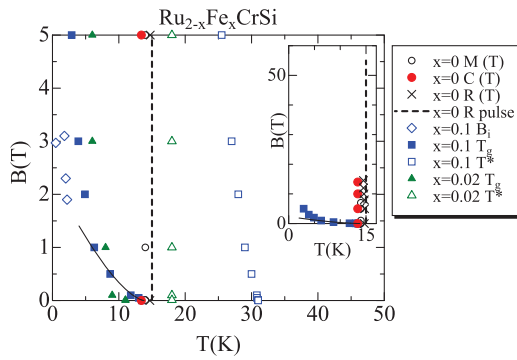


FIG. 11. Magnetic field vs temperature ($B - T$) magnetic phase diagram for $\text{Ru}_{2-x}\text{Fe}_x\text{CrSi}$ ($x = 0, 0.02, \text{ and } 0.1$). The antiferromagnetic (AF) transition T_N of Ru_2CrSi determined by magnetization (open circles), specific heat (solid circles), electrical resistance (crosses), and magnetoresistance in a pulsed field (MR), as described in Fig. 7(c) (broken line), is shown. The inset is the $B - T$ phase diagram extending to a high field of 55 T, where the almost upright phase boundary of the AF transition determined by MR is shown. Characteristic temperatures of the spin-glass behavior, T_g and T^* in magnetic fields, for $x = 0.1$ and 0.02 are plotted. Open diamonds show B_i for $x = 0.1$ determined from Figs. 8 and 9, and the solid line shows the expected dependence $\Delta T^{3/2} = [T_g(0) - T_g(B)]^{3/2}$ for the AT transition.

attributed to a relaxation. The result is a figure-8 loop. The strangest feature of the hysteresis behavior is the rather rapid decrease in $\rho(B)$ for increasing magnetic field (arrow 1), and it shows that the state of the substance is unpinned to the preceding state and is changing with respect to the pulsed field. Notably, this rapid decrease was unobserved in static fields, even as high as 18 T. These suggest that $\rho(B)$ under a pulsed field does not necessarily represent the equilibrium values of ρ at that field. For comparison, we show the result for a weaker pulsed field up to 7.8 T. Under this weak pulse, similar characteristics also appear (i.e., a figure-8 loop). This result suggests that these characteristics are independent of the magnitude of the pulse and are intrinsic. However, the $\rho(B)$ curve for decreasing B depends on the magnitude of the pulse, and even for increasing B it departs from the $\rho(B)$ curve for the 56 T pulse before the field reaches its maximum $B = 7.8$ T. One possible origin of the rapid decrease in $\rho(B)$ in pulsed fields with increasing B may be the rapid local increase in temperature in the initial stage in increasing B because the behavior of $\rho(T)$ is semiconducting [6, 11], and the increase in temperature may gradually relax after that. Nevertheless, this cannot account for all this behavior. The rapid extinction of the anomalous hysteresis above ~ 2.2 K seems difficult to attribute to the local increase in temperature. Figure 10(b) shows MRR under pulsed fields for $\text{Ru}_{1.7}\text{Fe}_{0.3}\text{CrSi}$ at temperatures between 1.3 and 30 K. Although it is similarly semiconducting with a weaker temperature dependence, anomalous behavior for $x = 0.1$ was not observed at all. Within experimental resolution in this measurement, hysteresis was unrecognized down to 1.3 K. Below 7 T it exhibits the largest negative MR in the series of $\text{Ru}_{2-x}\text{Fe}_x\text{CrSi}$ [11]. Nevertheless, in the higher-field region the slope of the decrease in $\rho(B)$ weakens and it exhibits a linear- B dependence, and the magnitude of

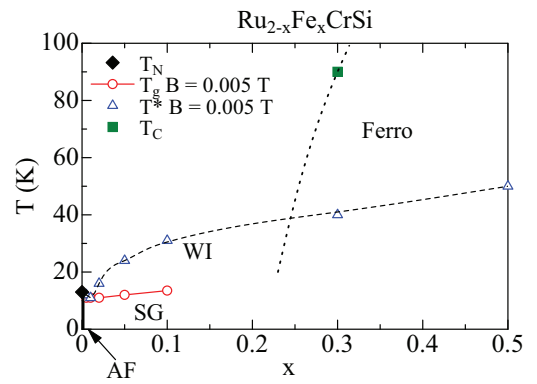


FIG. 12. Temperature vs Fe concentration ($T - x$) diagram for $\text{Ru}_{2-x}\text{Fe}_x\text{CrSi}$ ($0 \leq x \leq 0.5$). The solid diamond shows the antiferromagnetic (AF) transition T_N for $x = 0$. The AF phase exists only for near $x = 0$. Characteristic temperatures of spin-glass behavior, T_g [onset of strong irreversibility in $M(T)$] and T^* [maximum of $M(T)$], at a low field of $B = 0.005$ T are shown by open circles and triangles. Below T_g the spin-glass state with strong irreversibility (SG) exists, and for $T_g < T \lesssim T^*$ the inhomogeneous magnetic state with weak irreversibility (WI) exists. The ferromagnetic transition T_C is shown by the solid square (T_C for $x = 0.5$ is 190 K).

MRR at 45 T is $\sim 30\%$, as large as for $x = 0.1$. This conforms to a proposition that the ferromagnetism for $x = 0.3$ is inhomogeneous, and the large MR in lower fields is due to an alignment of the inhomogeneous ferromagnetic regions, inducing a decrease in boundary scattering.

The origins of negative MR in Fe-substituted samples may be randomness and magnetic scattering induced by Fe by considering MR changes from positive to negative with the introduction of Fe. Unsaturated negative MR, which is almost linear in B in the high-field region and is supposed to continue to a higher field, was observed for $x = 0.1$ and 0.3 . This is considered to be related to unsaturated $M(B)$ (Fig. 5) that gradually suppresses the magnetic scattering with increasing B . Meanwhile, in the antiferromagnetic Ru_2CrSi , such a magnetic scattering effect for negative MR is absent, and the effect of magnetic scattering related to the AF order is small.

IV. DISCUSSION

To summarize and discuss the results, the $B - T$ and $T - x$ magnetic phase diagrams are shown in Figs. 11 and 12.

In Ru_2CrSi , the results for specific heat and μSR measurements showed that it is indeed a thermodynamic and magnetic phase transition, in contrast with the behavior in $\text{Ru}_{1.9}\text{Fe}_{0.1}\text{CrSi}$. T_N in magnetic fields determined from these measurements is plotted in Fig. 11. As shown by the broken line in Fig. 11 in the inset, the phase boundary of the AF transition is almost upright up to 55 T. Therefore, B_0 , the critical field of the transition from the AF phase at $T = 0$ K, appears very high. Considering that T_N is as low as 13 K, this behavior seems very unusual, because if the AF phase is a usual AF phase derived from local moments, $k_B T_N \sim \mu_m B_0$ holds, where k_B and μ_m are the Boltzmann constant and the value of the ordered local magnetic moment, respectively. Although μ_m was unknown in Ru_2CrSi , it is reasonable to

assume μ_m to be $\sim 2\mu_B$ because the paramagnetic moment is estimated to be $2.28\mu_B$ [15], and further in Ru_2CrGe , which is almost identical in magnetic properties for Ru_2CrSi , in the AF phase the magnetic moment is carried by Cr and its moment was estimated to be $1.8\mu_B$ [10]. With these values, B_0 is estimated to be ~ 10 T, and this contradicts the experimental fact.

The AF transition unchanged to the magnetic field has been reported in other materials, such as the Heusler-type compound Mn_3Si [20], the half-Heusler-type compound CuMnSb [21], and CrB_2 [22]. Also, measurements for these in pulsed fields were performed, and the absence of a transition to high fields is suggested [27]. The robustness to magnetic field in these materials was explained by band effects. The $\rho(T)$ dip around the transition is reminiscent of the resistivity of Cr at the spin density wave (SDW) transition [28,29], and it suggests a change in the electronic structure around T_N in Ru_2CrSi . Similar behavior was also reported for the half-Heusler compound GdPtBi [30] or Fe pnictides such as $\text{Ba}(\text{Fe}_{1-x}\text{Mn}_x)_2\text{As}$, which shows SDW and glassy behavior [31].

Figure 12 shows the T versus x (Fe content) diagram for $0 \leq x \leq 0.5$. For $0.3 \lesssim x \lesssim 0.5$, ferromagnetism, which is presumed to be inhomogeneous, was observed. Although the inhomogeneous ferromagnetic phase may be considered to be like a Griffiths phase [32], in our analysis the magnetic susceptibility showed no temperature dependence expected of a Griffiths phase, that is, the susceptibility increases over the Curie-Weiss law at low fields [24]. Notably, the Griffiths phase picture is not always applied for inhomogeneous ferromagnetism [33]. Below $x \sim 0.2$, spontaneous magnetization disappears, and in $\text{Ru}_{1.9}\text{Fe}_{0.1}\text{CrSi}$ the formation of an inhomogeneous magnetic state and spin freezing occur, inducing the behavior of successive SG transitions at T_g (spin freezing) and T^* (gradual formation of a magnetic frozen region), as fully explained in Refs. [11,13]. This behavior is also observed for $0.3 \lesssim x \lesssim 0.5$ [12], where several magnetic phases may coexist. By decreasing x further, T^* decreases, whereas T_g (~ 15 K) changes slightly, and they appear to meet around $x \sim 0.01$. It appears that T_g and T^* become T_N at $x \sim 0$, where a true AF transition occurs. Notably, T^* increases with Fe substitution, which is assumed to bring about a ferromagnetic interaction and accordingly to increase magnetization, whereas T^* is considered a measure of the AF interaction; these two points would seem to contradict each other. Nevertheless, these x dependences suggest the strong relationship of the AF transition and SG behavior with the anomalies at T_N and T_g .

In Fig. 11, phase boundaries in a magnetic field for $x = 0.02$ and 0.1 , in addition to $x = 0$, are shown. For 0.1 and 0.02 , $T_g(B)$ in a magnetic field determined from $M(T)$ are shown, and they are similar. Although the nature of the SG transition in a magnetic field remains controversial [34], the SG transition in a magnetic field has often been described in terms of the de Almeida–Thouless (AT) transition [35]. The SG below T_g exhibits characteristics expected of the AT phase; strong irreversibility exists between the $M(T)$ curves for ZFC and FC, and the T_g extrapolated to 0 T agrees with the spin-freezing temperature $T_g(0)$ revealed by μSR . The relationship of T_g with magnetic fields deduced from $M(T)$ follows the expected

form for the AT line $B \propto (\Delta T)^{3/2} = [T_g(0) - T_g(B)]^{3/2}$ at low fields, as shown in Fig. 11 by the solid line, where $T_g(0)$ is supposed to be 15 K [11,35]. Moreover, B_i determined from hysteresis in $\rho(B)$ [Figs. 8(a) and 9(b)] is plotted. B_i shows similar behavior to that of $T_g(B)$, although B_i at the lowest temperature 0.5 K is almost the same as that at 1.3 K. However, even if the AT transition is realized, the high-field behavior probably has not yet been understood both experimentally and theoretically. Nevertheless, we believe that this unusual hysteresis is a manifestation of the strong irreversibility in SG, like that described in the AT theory. Meanwhile, T^* seems not to depend much on B . We investigated other x and found that the magnetic field dependences of T^* and T_g are basically the same for $0 < x \leq 0.1$ [7]. This behavior may be interpreted as successive SG transitions. Successive SG transitions in the Heisenberg spin system are proposed by the AT and GT (Gabay–Toulouse) theory [36,37], and actually the magnetic phase diagram of the transitions resembles that of the AT and GT lines. In particular, the transition at T_g has AT-like character. Meanwhile, the anomaly at T^* does not show properties proposed as the GT transition, but rather a crossover in which sporadic magnetic frozen regions, probably antiferromagnetic, occur gradually. This looks like a situation described by an AF Griffiths phase model. However, the criterion for judging an AF Griffiths phase seems not to be established and is only qualitatively understood [31]. To explain this phase diagram, a model of two components, which are rather independent but are linked, is presented. Following the AT and GT theories, we tentatively call the two components longitudinal and transverse components. The longitudinal component freezes at T_g . The transverse component has greater susceptibility and a preference for an ordered state, and it increases with x . This may cause the increase in the magnitudes of M and T^* . Meanwhile, the longitudinal component has a smaller susceptibility and freezes randomly around constant temperature T_g . At $x \lesssim 0.01$, the transverse component makes a stronger link with the longitudinal components, and the AF long-range order develops. This is just a qualitative picture, and the terms longitudinal and transverse are intangible, which might indicate spacious regions.

Next, we consider the bizarre hysteresis in MR for $x = 0.1$. Considering that the bizarre hysteresis under static and pulsed fields has only been seen at limited low temperatures and has probably only been observed for $x = 0.1$, it is regarded as an intrinsic phenomenon. Since the size and appearance of the hysteresis behaviors differ greatly between static and pulsed fields, they cannot be regarded as the same phenomenon. Nevertheless, both unusual behaviors after ZFC are interpreted as manifestations of strong irreversibility accompanying the SG. The behavior in pulsed fields at least may be attributed partly to the enhanced relaxation time that is generally considered to accompany glassy states. Nevertheless, this behavior is very special; we are not aware of any similar behavior of bizarre hysteresis in pulsed fields in other materials. Additionally, in the magnetization $M(B)$ under a pulsed field, the unusual hysteresis was unobserved in the scale of Fig. 5, whereas in $M(B)$ in a static field, a relatively small hysteresis, probably due to SG, was observed at low temperatures below 4 K [11].

The salient hysteresis in $\rho(B)$ for $x = 0.1$ appears not to be related with $M(B)$.

One hypothesis for this behavior is that after ZFC below T_g , the SG state with strong irreversibility occurs, which we tentatively call the AT state, and this AT state is supposed to have lower electrical resistivity than that in the high-field state, judging from the smaller values of $\rho(B)$ in the static field initially after ZFC, as shown by arrow 1 in Fig. 8(a). In the higher-field region, this state may persist and low resistivity is probably enhanced, thereby inducing a rapid decrease in $\rho(B)$ with increasing B . The unusual hysteresis is only visible at temperatures below ~ 3 K, which is much lower than $T_g = 15$ K. A possible explanation is that the AT line [$T_g(B)$] strongly depends on B in the lower B region, and thus the AT region in the magnetic field extends only in limited low temperatures. A figure-8 behavior of MR was reported in HoFe_4Ge_2 in a static field [38]. In this case, the first-order phase transition seems to be related to the behavior, which differs from the present case. However, it is specified that the enhanced relaxation time attributed to kinetic arrest in that case might correspond with what occurs in the present case.

In this series of compounds, unique aspects of the AF state and the SG state characterized by strong irreversibility and inhomogeneity are clarified. However, more studies are still needed to understand the underlining physics.

V. CONCLUSIONS

Magnetic and thermodynamic properties, resistivity in a magnetic field, particularly for properties in a high magnetic field, and μSR studies were performed for $\text{Ru}_{2-x}\text{Fe}_x\text{CrSi}$. In Ru_2CrSi , an antiferromagnetic transition occurs at $T_N = 13$ K,

where a clear dip in the temperature dependence of resistivity is observed. The temperature at the dip remains constant up to 55 T, and magnetization is proportional to B up to 55 T. The specific heat shows a peak at the temperature T_N . The shape of the specific heat and T_N remain constant up to 14 T. These show the robustness of the antiferromagnetic state to the magnetic field, suggesting that this transition is related to the electronic band structure. Meanwhile, $\text{Ru}_{1.9}\text{Fe}_{0.1}\text{CrSi}$ exhibits the behavior of successive SG transitions. The properties for $0 \leq x \leq 0.1$ suggest a deep relation between the antiferromagnetism and the SG behavior.

For magnetoresistance in a high field, while Ru_2CrSi shows a positive magnetoresistance, $\text{Ru}_{1.9}\text{Fe}_{0.1}\text{CrSi}$ exhibits a negative magnetoresistance, and the remarkable behavior is the unusual hysteresis at low temperature in ZFC conditions, specifically in pulsed fields. This must originate in the SG state with strong irreversibility.

ACKNOWLEDGMENTS

Part of this work was carried out by the joint research in the Institute for Solid State Physics, the University of Tokyo (ISSP), and we are grateful to T. Yamauchi at the Materials Design and Characterization Laboratory, ISSP for advice and help. Part of this work was performed at High Field Laboratory for Superconducting Materials, Institute for Materials Research, Tohoku University (Projects No. 18H0017 and No. 19H0025). Parts of the measurements were performed using the PPMS of Institute of Pulsed Power Science, Kumamoto University. M.H. acknowledges support from JSPS KAKENHI Grant No. 17K06774.

-
- [1] C. Felser, G. Fecher, and B. Balke, *Angew. Chem. Int. Ed.* **46**, 668 (2007).
- [2] M. I. Katsnelson, V. Y. Irkhin, L. Chioncel, A. I. Lichtenstein, and R. A. de Groot, *Rev. Mod. Phys.* **80**, 315 (2008).
- [3] S. Ishida, S. Fujii, S. Kashiwagi, and S. Asano, *J. Phys. Soc. Jpn.* **64**, 2152 (1995).
- [4] S. Mizutani, S. Ishida, S. Fujii, and S. Asano, *Mater. Trans.* **47**, 25 (2006).
- [5] K. Matsuda, M. Hiroi, and M. Kawakami, *J. Phys.: Condens. Matter* **17**, 5889 (2005); **18**, 1837(E) (2006).
- [6] M. Hiroi, K. Matsuda, and T. Rukkaku, *Phys. Rev. B* **76**, 132401 (2007).
- [7] M. Hiroi, H. Ko, S. Nakashima, I. Shigeta, M. Ito, H. Manaka, and N. Terada, *J. Phys.: Conf. Ser.* **400**, 032020 (2012).
- [8] M. Hiroi, K. Uchida, I. Shigeta, M. Ito, K. Koyama, S. Kimura, and K. Watanabe, *J. Korean Phys. Soc.* **62**, 2068 (2013).
- [9] M. Hiroi, S. Nakashima, K. Nakao, T. Rukkaku, M. Ito, I. Shigeta, H. Manaka, and N. Terada, *J. Supercond. Novel Magn.* **24**, 753 (2011).
- [10] P. J. Brown, A. P. Gandy, T. Kanomata, Y. Kusakari, A. Sheikhi, K.-U. Neumann, B. Ouladdiaf, and K. R. A. Ziebeck, *J. Phys.: Condens. Matter* **20**, 455201 (2008).
- [11] M. Hiroi, T. Rukkaku, K. Matsuda, T. Hisamatsu, I. Shigeta, M. Ito, T. Sakon, K. Koyama, K. Watanabe, S. Nakamura, T. Nojima, T. Nakano, L. Chen, T. Fujiwara, Y. Uwatoko, H. Manaka, and N. Terada, *Phys. Rev. B* **79**, 224423 (2009).
- [12] M. Ito, T. Hisamatsu, T. Rukkaku, I. Shigeta, H. Manaka, N. Terada, and M. Hiroi, *Phys. Rev. B* **82**, 024406 (2010).
- [13] M. Hiroi, T. Hisamatsu, T. Suzuki, K. Ohishi, Y. Ishii, and I. Watanabe, *Phys. Rev. B* **88**, 024409 (2013).
- [14] S. Nishiinoue, H. Suwa, I. Shigeta, M. Hiroi, K. Koyama, S. Kimura, K. Watanabe, and M. Fujii, *JPS Conf. Proc.* **3**, 017018 (2014).
- [15] M. Hiroi, H. Sano, T. Tazoko, I. Shigeta, M. Ito, K. Koyama, H. Manaka, N. Terada, M. Fujii, A. Kondo, and K. Kindo, *J. Alloys Compd.* **694**, 1376 (2017).
- [16] T. Matsuzaki, K. Ishida, K. Nagamine, I. Watanabe, G. Eaton, and W. Williams, *Nucl. Instrum. Methods Phys. Res. Sec. A* **465**, 365 (2001).
- [17] M. Ito, T. Hisamatsu, S. Nakashima, I. Shigeta, K. Matsubayashi, Y. Uwatoko, and M. Hiroi, *J. Phys.: Conf. Ser.* **266**, 012011 (2011).
- [18] K. Li, S. Jin, J. Guo, Y. Xu, Y. Su, E. Feng, Y. Liu, S. Zhou, T. Ying, S. Li, Z. Wang, G. Chen, and X. Chen, *Phys. Rev. B* **99**, 054421 (2019).
- [19] S. Nakatsuji, H. Tonomura, K. Onuma, Y. Nambu, O. Sakai, Y.

- Maeno, R. T. Macaluso, and J. Y. Chan, *Phys. Rev. Lett.* **99**, 157203 (2007).
- [20] C. Pfleiderer, J. Bœuf, and H. v. Löhneysen, *Phys. Rev. B* **65**, 172404 (2002).
- [21] J. Bœuf, C. Pfleiderer, and A. Faißt, *Phys. Rev. B* **74**, 024428 (2006).
- [22] A. Bauer, A. Regnat, C. G. F. Blum, S. Gottlieb-Schönmeyer, B. Pedersen, M. Meven, S. Wurmehl, J. Kuneš, and C. Pfleiderer, *Phys. Rev. B* **90**, 064414 (2014).
- [23] I. Watanabe, T. Adachi, K. Takahashi, S. Yairi, Y. Koike, and K. Nagamine, *Phys. Rev. B* **65**, 180516(R) (2002).
- [24] Y. Shimada, S. Miyasaka, R. Kumai, and Y. Tokura, *Phys. Rev. B* **73**, 134424 (2006).
- [25] S. Tsubouchi, T. Kyômen, M. Itoh, P. Ganguly, M. Oguni, Y. Shimojo, Y. Morii, and Y. Ishii, *Phys. Rev. B* **66**, 052418 (2002).
- [26] S. Senoussi and Y. Öner, *J. Appl. Phys.* **55**, 1472 (1984).
- [27] M. Doerr, J. Buf, C. Pfleiderer, M. Rotter, N. Kozlova, D. Eckert, P. Kersch, K.-H. Müller, and M. Loewenhaupt, *Phys. B: Condens. Matter* **346-347**, 137 (2004), proceedings of the 7th International Symposium on Research in High Magnetic Fields.
- [28] E. Fawcett, *Rev. Mod. Phys.* **60**, 209 (1988).
- [29] E. Fawcett, H. L. Alberts, V. Y. Galkin, D. R. Noakes, and J. V. Yakhmi, *Rev. Mod. Phys.* **66**, 25 (1994).
- [30] T. Suzuki, R. Chisnell, A. Devarakonda, Y.-T. Liu, W. Feng, D. Xiao, J. Lynn, and J. Checkelsky, *Nat. Phys.* **12**, 1119 (2016).
- [31] D. S. Inosov, G. Friemel, J. T. Park, A. C. Walters, Y. Texier, Y. Laplace, J. Bobroff, V. Hinkov, D. L. Sun, Y. Liu, R. Khasanov, K. Sedlak, P. Bourges, Y. Sidis, A. Ivanov, C. T. Lin, T. Keller, and B. Keimer, *Phys. Rev. B* **87**, 224425 (2013).
- [32] R. B. Griffiths, *Phys. Rev. Lett.* **23**, 17 (1969).
- [33] C. He, M. A. Torija, J. Wu, J. W. Lynn, H. Zheng, J. F. Mitchell, and C. Leighton, *Phys. Rev. B* **76**, 014401 (2007).
- [34] Y. Tabata, T. Waki, and H. Nakamura, *Phys. Rev. B* **96**, 184406 (2017).
- [35] J. R. L. de Almeida and D. J. Thouless, *J. Phys. A* **11**, 983 (1978).
- [36] M. Gabay and G. Toulouse, *Phys. Rev. Lett.* **47**, 201 (1981).
- [37] D. M. Cragg, D. Sherrington, and M. Gabay, *Phys. Rev. Lett.* **49**, 158 (1982).
- [38] J. Liu, V. Pecharsky, and K. Gschneidner, *J. Alloys Compd.* **631**, 26 (2015).